

# Defect profiling in semiconductor layers by electrochemical method

© Ákos Nemcsics<sup>¶</sup>, János P. Makai

Hungarian Academy of Sciences, Research Institute for Technical Physics and Materials Science,  
H-1525 Budapest, Hungary

(Получена 18 сентября 2002 г. Принята к печати 4 декабря 2002 г.)

A special selective electrochemical etching based equipment is presented which is appropriate for in-situ observation of the defect structure. The working of the set-up is demonstrated on the InGaAs/GaAs (001) heteroepitaxial systems where the epitaxial layer thickness was above the critical layer thickness. By incremental layer removal, the depth profile on the dislocation density was mapped. The measured defects density is inversely proportional to the layer thickness and corresponds to theoretical model.

## 1. Introduction

It is of high interest to understand the behaviour of the defects induced by the lattice misfit in heteroepitaxial systems [1]. The defects in the layers can be investigated by different methods. One of the common methods for the defect distribution is X-ray topography. Its main advantage is that the different kinds of defects can be investigated in a non-destructive way. The disadvantages are that the investigation is confined only to lateral direction and the measurement is very time consuming. Another commonly used method is the transmission electron microscopy. The defect distribution in the cross sectional direction can be investigated in high resolution with this method. The investigation is limited also to one direction and the sample preparation is a cumbersome and time consuming procedure. We show in this work an equipment based on electrochemical method, which is appropriate for simple and quick investigation of crystal defects both in lateral and vertical directions, too.

Using electrolyte on the semiconductor surface, a controlled electrochemical layer removal can be carried out. The selective electrochemical etching is a widely used method for the investigation of defects in the epitaxial layers and substrate material. One of the advantages of this method is that it provides defect distribution both in lateral [2] and vertical [3] directions. It shows none of the disadvantages of the other methods: it is a fast method with good resolution, furthermore the set-up is simple.

In this study, we look at the threading defects in  $\text{In}_x\text{Ga}_{1-x}\text{As}/\text{GaAs}$  heterostructures grown by molecular beam epitaxy (MBE) by using selective electrochemical etching. The electrochemical defect profiling is carried out with the help of a novel electrochemical defect profiler. By incremental etching, we map the depth distribution of the defects. The results obtained are compared with a theoretical model.

## 2. The equipment

### 2.1. General description

The electrochemical defect developer consists of two main parts. One of them is the electrochemical part, the other is the optical one. The block scheme of the whole setup is shown in Fig. 1. The electrochemical part consists of a specially constructed electrochemical cell. The electrochemical cell is connected to a potentiostat type Elektroflex EF451 [4]. The potentiostat is controlled by a computer where the connection is realised by a special interface card (EF3506) through parallel port. The maximal output voltage is  $\pm 20$  V. The current can be measured in 8 ranges from 2 A to 25 pA. The stat is controlled entirely digitally where the status of the equipment is displayed by lighting diodes on the front panel. The control program written in Turbo Pascal makes different working modes possible such as cyclic voltammetry, impedance analysis and integral of current. The program makes automatically a measurement report and attaches it to the measured data and the setting parameters of the set-up. A printer serves for the printing of the measured diagrams. The electrolyte

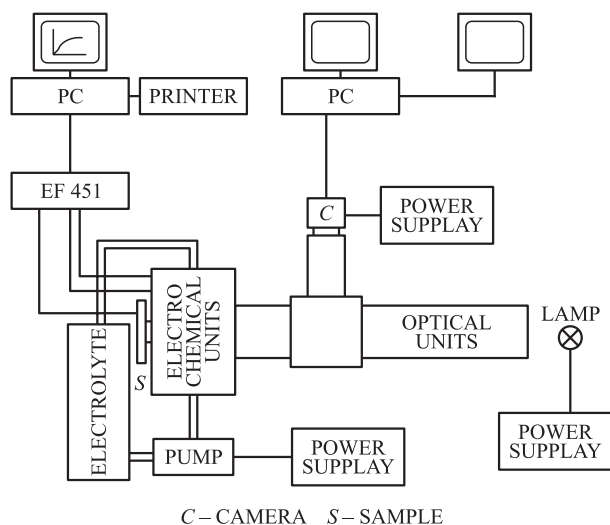
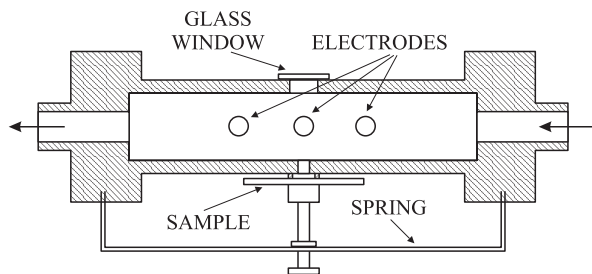


Figure 1. The block scheme of the electrochemical defect profiler.

<sup>¶</sup> E-mail: nemcsics@mfa.kfki.hu



**Figure 2.** Cross section of the special designed electrochemical cell.

in the specially designed electrochemical cell is circulated by the help of a pump.

The optical part consists of a lens system building most of the illuminating part, a microscope objective and a beam splitter being parts of both the illuminating and viewing parts and an attached CCD camera, manufactured by Sony. The case of the optical system was manufactured from an aluminum block. The adjustment of the optics can be carried out by the help of screws. The attached camera is connected to a computer with two monitors (one of them serves for the menu of the image processing program and the other one for the visualisation of the investigated surface). The picture can be saved as a bmp file.

## 2.2. The electrochemical unit

One of the most important parts of the setup is the specially designed electrochemical cell. The cell must be of low depth that is the sample has to be close to the window because of the limited working distance of the optical observation. The construction is also special concerning the small cross section. The cell is cut from a plexi glass block. The specially constructed electrochemical cell is shown in Fig. 2.

The arrangement of our electrochemical measuring setup is often used in electrochemical investigations. The working electrode is the semiconductor sample, the counter electrode is made of carbon and platinum wire, and the reference electrode is a saturated calomel electrode [5]. The sample is held against a rubber ring seal of 3 mm diameter.

The narrow cell needs special method for the removal of bubble and cleaning of chamber from the electrolyte. Because the size of cell is small the fresh electrolyte which is needed to the reaction is transported by circulation with the help of an attached pump. The pump serves furthermore for the removal of the bubbles, which might stuck in the sealing ring and for the cleaning of cell by distilled water.

The electrochemical layer removal is carried out under two different conditions. One of them is the so called polishing or non-selective condition where the bias is chosen on the low-slope-part of the polarization curve with optical stimulation. The another is the selective etching that can be carried out by very small polarization under lightly illuminated surface or at large polarization in darkness. The

crossed charges are integrated during the etching so the removed layer thickness was calculated by Faraday's law [6] where the entering parameters are the physical (material density, valence number etc.) and geometrical data of the system. The etched depth is controlled by alpha-step profiler.

## 2.3. The optical unit

The optical layout of the illuminating and viewing system is shown on Fig. 3. For simplicity the figure does not include the etching chamber only the wafer. A 250 W tungsten halogen lamp is used as the light source. It can be considered as about a 3200 K planckian radiator in the wavelength range of 0.3 to  $2.5\mu\text{m}$  if used at nominal values and can be tested by special probes [7,8]. Either broad band or narrow band illumination can be applied to the wafer. The spectral limiting media of the broadband illumination is the liquid in the etching chamber, if it is water based the transmission is between 0.3 and  $1.4\mu\text{m}$  which is much stricter than the limitation of the glass material of the lenses or the light source. Even this about 10 mm thick water absorbs the radiation above  $1.4\mu\text{m}$  drastically, the transmission is only a fraction of a percent. This spectral range is only slightly wider than the sensitive range of the Si CCD camera. within this spectral range a narrow band can be selected by inserting interference filters ( $F$ ) to investigate the effect of etching as a function of the illuminating wavelength.

A magnified image of the lamp is produced by the lens  $L1$  on the lens  $L2$ . The lens pair  $L2$  and  $L3$  images, again magnified,  $L1$  to the lens  $L4$ , that is further imaged by the reflective microscope objective  $RO$  to the wafer  $W$ .  $L4$  images  $L3$  onto the convex mirror of the objective. An image of the wafer is produced on the camera by the microscope objective through the beam splitter  $BS$ . A reflective microscope objective was chosen because it has a high working distance of about 15 mm providing room for the etching chamber. The magnification of the objective is 15, since the usable diameter of the lenses is 20 mm, this means a light spot diameter of 1.33 mm on the wafer. About half of this area is imaged to the active surface of the detector. The uniformity of the light spot on the wafer is ensured by imaging the uniformly illuminated  $L1$  to the wafer. The numerical aperture of the objective is 0.28 that provides an optical resolution, according to the Raleigh criteria, of  $0.65\mu\text{m}$  at the wavelength of 300 nm,  $1.42\mu\text{m}$  at 650 nm and  $2.18\mu\text{m}$  at 1000 nm. This suggests to do the

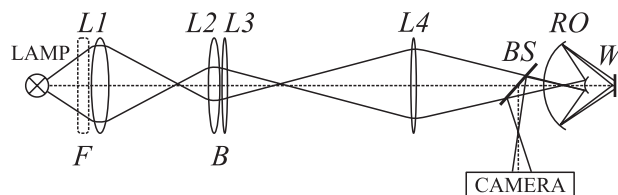


**Figure 3.** Schematic draw of the optical system where  $L1-L4$  are lenses,  $RO$  is microscope objective and  $BS$  is beam splitter.

etching at the desired wavelength or wavelength band and to shoot a picture at the shortest wavelength facilitated by the spectral emittance of the source and the sensitivity of the Si CCD camera. The pixel size of the used camera is about  $10 \times 10 \mu\text{m}^2$ , that means that the optical resolution of the objective times the magnification ( $0.65 \times 15 \mu\text{m}^2$ ), at the short wavelength edge, corresponds to the mechanical size of a single pixel. The disadvantage of the reflective objective is that the axial quasi parallel rays reaching the middle portion of the convex mirror of the objective reflect straight back to the camera through the beam splitter (*BS*) that would blind the camera. To inhibit this a small opaque disc *B* is mounted in between *L2* and *L3* blocking these rays. The beam splitter is of a pellicle type that ensures a single image of the wafer on the camera produced by the objective.

Since the camera has no objective there is no automatic iris adjustment, it is replaced either by the proper selection of the lamp current or by the translation of the lamp. Changing the current will change the so-called distribution temperature of the lamp but if narrow spectral band illumination is used this does not cause any deviation from the ideal etching conditions. If broad band illumination is applied, the changing of the lamp current changes the spectral composition of the illumination, too, therefore the translation method has to be used. This ensures that no overflow of the CCD camera occurs. The lamp is mounted on an *XYZ* translation stage, the etching chamber on an *XY* one. The vertical *Z* motion is provided by the adjustment of the whole optic that is placed in a tube.

The camera is a black and white one having  $512 \times 512$  pixels. It is connected to a frame grabber that allows further manipulation, for example comparison of images, convolution, etc. It permits the simultaneous display of the buffer frame and an overlayable colour graphics plane, as well as management of programmer accesses. It has online preprocessing units through its look up tables, located at the input and output of the video channels. A real time conversion is provided by a flash converter having a resolution of 8 bits.

### 3. Experiment and discussion

#### 3.1. Selective electrochemical etching

The GaAs (001) oriented wafers used in the experiment are Zn doped ( $p = 4 \times 10^{18} \text{cm}^{-3}$ ) where the etch pit density of EPD  $< 5 \times 10^4 \text{cm}^{-2}$ . The In content in the MBE grown layer was 30% and the layer thickness was  $1.2 \mu\text{m}$ . The sample preparation is detailed in Ref. [9]. By using electrochemical etching we found that the undoped layers were of slightly *p*-type. The Matthews–Blakeslee (equilibrium) critical layer thickness for the misfit generating dislocation [1] is about 8 nm for the sample ( $\text{In}_{0.3}\text{Ga}_{0.7}\text{As}/\text{GaAs}$ , lattice misfit  $f = 0.024$ ), that is to say our layer is much thicker than the critical layer thickness.

The morphology of the etched surface was observed by our own optical system. The removed layer thickness was calculated by Faraday's law and controlled by a surface stylus profiler. The EPD values were determined with defect counter on the screen, which corresponds to an area of about  $586 \times 440 \mu\text{m}^2$  on the surface.

The etching parameters (e.g. bias voltage) were optimized by using a bare GaAs substrate. According to our former experiments 10%  $\text{NH}_4\text{OH}$  is a suitable aqueous electrolyte for defect etching [8,11]. Besides the type of electrolyte, the surface morphology depends on the bias voltage, too. After etching, the surface is well structured when larger than 0.5 V anodic bias (defect etch conditions) is applied. At lower bias voltage, the surface remains mirror-like (polish etch conditions). The etching current, when the bias ranges between 0.5 and 0.8 V is stable, i.e., increases only slowly with depth or time. The etching current is large at higher doping in this bias range, and the etching rate is low. In this range we can remove thick layers and detect the location of the etched surface relative to interface or substrate. At anodic bias larger than 1 V the etching current becomes unstable and increases strongly with time/depth. In this etching current range for the undoped layer it is larger than for the bare substrate. The slope of *I*–*V* characteristics of the epitaxial layer, above 0.5 V bias, is larger than the slope of the of the substrate. This can be explained by the presence of defects. At higher EPD the current versus time/depth is steeper since at higher bias voltage current filaments are formed at the imperfections [2].

Based on these results, we carried out the defect etching at about 0.6 V bias, where the current density was less than  $2 \text{mA}/\text{cm}^2$ . Prior to studying the substrate, the damaged surface layer was removed by non-selective etching. The position of the interface is indicated by current vs. depth function. The current density has a sudden increment at the interface, because the substrate has higher charge carrier concentration than the epilayer (see Fig. 2 in [3]).

#### 3.2. Comparison with model

Typical picture of the surface morphology for sample after selective etching is shown in Fig. 4. The measured EPD of the substrate was about half of the value specified by the supplier. The substrate defect density was found to be non-uniform. This indicates that the epilayer dislocations originate even from sources other than the grown-dislocations of the substrate. We further note that the non-uniform distribution of the threading dislocation is inherent to the mismatched systems. The average measured EPD vs. depth data are depicted on Fig. 5. The size of the etch pits are different; larger pits indicate dislocations traveling further away from the interface; this is an indirect evidence for the depth inhomogeneity of the defect density. The elongated shape of the pits is due to the higher etch rate along one of the [011] axes.

Several theoretical models have been elaborated to predict the threading dislocation density *D* in mismatched het-

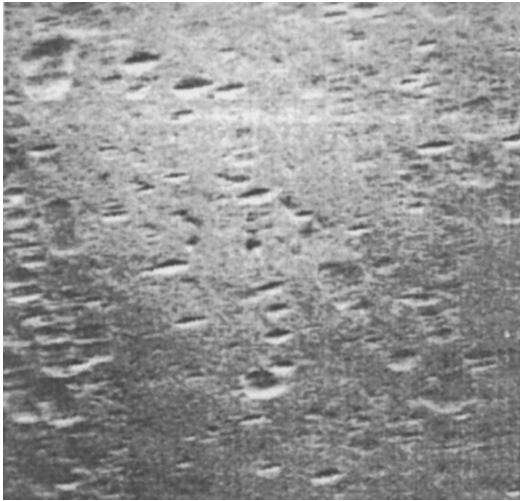


**Figure 4.** View of the etched surface at  $0.7\ \mu\text{m}$  from the interface where the EPD is about  $2 \times 10^8\ \text{cm}^{-2}$ .

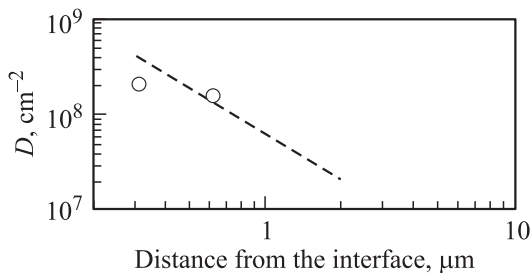


**Figure 5.** The threading dislocation density  $D$  (symbols) as a function of etched depth for the measured sample with model calculation (dashed line).

eroepitaxial systems [1]. The threading dislocation densities determined by defect development are generally smaller than the theoretically predicted values [3,12]. Wehmann et al. have been introduced another model for the determination of the threading dislocation density [13]. The values predicted by this model agree very well with the measured EPD on the thick highly mismatched heteroepitaxial structures [12]. In our case the calculated curve is drawn by solid line in Fig. 5 which corresponds to the depicted data.

## 4. Conclusions

A novel electrochemical equipment for defect investigation was presented. The set-up is suitable for observation of defect distribution in lateral and vertical direction, too. The specially constructed electrochemical cell and optical system were detailed. The investigated material system was thick InGaAs/GaAs heterostructure. It has been shown that the presented set-up for selective electrochemical etching is suitable for depth-dependent study of defect density in lattice-mismatched heteroepitaxial systems. The results

agree with the general physical picture of heteroepitaxial growth and relaxation processes.

The authors are indebted to L. Dobos (Elektroflex), T. Pajkossy, Zs. Kerner and M. Rácz for helpful discussion and for their hardware and software contribution to making the present setup. This work and the realisation of the equipment was funded by the Hungarian National Scientific Foundation (OTKA) through Grants T 030426 and E 039453.

## References

- [1] E.A. Fitzgerald. *Mater. Sci. Rep.*, **7**, 87 (1991).
- [2] Á. Nemcsics, L. Petrás, K. Somogyi. *Vacuum*, **41**, 1015 (1990).
- [3] Á. Nemcsics, F. Riesz, L. Dobos. *Thin Sol. Films*, **343–344**, 520 (1999).
- [4] www.elektroflex.hu (elektroflex@deltav.hu).
- [5] M.M. Faktor, J.L. Stevenson. *J. Electrochem. Soc.*, **125**, 621 (1978).
- [6] T. Ambridge, M.M. Fakrot. *J. Appl. Electrochem.*, **5**, 319 (1975).
- [7] M. Rácz, I. Réti, S. Ferenczi. *Opt. Eng.*, **32**, 2517 (1993).
- [8] M. Rácz, I. Réti, S. Ferenczi. *Proc. Int. Conf. „Photodetectors and Power Meters“*, July 15–16, 1993 (San Diego, California). [SPIE, **2022**, 192 (1993)].
- [9] Á. Nemcsics, J. Olde, M. Geyer, R. Schnurpfeil, R. Manzke, M. Skibowski. *Phys. St. Sol. (a)*, **155**, 427 (1996).
- [10] Á. Nemcsics, K. Somogyi. *Acta Phys. Hung.*, **70**, 259 (1991).
- [11] Á. Nemcsics, M. Schuszter, L. Dobos, Gy. Ballai. *Mater. Sci. Eng. B*, **90**, 67 (2002).
- [12] H.H. Wehmann. *Habilitationschrift, TU Carolo-Wilhemina zu Braunschweig*, 2000.
- [13] H.H. Wehmann, G.P. Tang, A. Schlachetzki. *Sol. St. Phenomena*, **32–33** 445 (1993).

Редактор Т.А. Полянская